Monthly Notices
of the
ROYAL ASTRONOMICAL SOCIETY

MNRAS **450,** 223–228 (2015) doi:10.1093/mnras/stv375

Radiative lifetimes and transition probabilities in Rh I

G. Malcheva,[1] L. Engström,[2] H. Lundberg,[2] H. Nilsson,[4] H. Hartman,[3,4] K. Blagoev,[1⋆] P. Palmeri[5] and P. Quinet[5,6]

[1]*Institute of Solid State Physics, Bulgarian Academy of Sciences, 72 Tzarigradsko Chaussee, BG - 1784 Sofia, Bulgaria*
[2]*Department of Physics, Lund University, PO Box 118, SE-221 00 Lund, Sweden*
[3]*Applied Mathematics and Material Science, Malmö University, SE-20506 Malmö, Sweden*
[4]*Lund Observatory, Lund University, PO Box 43, SE-221 00 Lund, Sweden*
[5]*Astrophysique et Spectroscopie, Université de Mons, B-7000 Mons, Belgium*
[6]*IPNAS, Université de Liège, B-4000 Liège, Belgium*

Accepted 2015 February 19. Received 2015 January 29; in original form 2014 November 04

ABSTRACT

Radiative lifetimes of 17 high-lying excited states in Rh I are measured using the time-resolved laser-induced fluorescence method. Out of these lifetimes, 13 are new and the remaining four confirm previous measurements. Furthermore, we report the first theoretical investigation of Rh I, where the radiative decay properties of all experimentally known levels below 47 000 cm^{-1} are calculated using a pseudo-relativistic Hartree–Fock method including core polarization effects. The theoretical calculations are found to be in very good agreement with the experimental results. A large set of new transition probabilities is presented for lines of astrophysical interest in the spectral range 2200–10 000 Å.

Key words: atomic data – atomic processes – methods: laboratory: atomic.

1 INTRODUCTION

Rhodium is one of the refractory elements observed in the solar photosphere and in meteorites (Cameron 1981). To determine abundances, the intrinsic transition probability (*A*-value) or oscillator strength (*f*-value) must be known for the observed lines. Experimentally, the best and most widely used technique to obtain these values is to combine branching fractions, i.e. the intensity of one line divided by the sum of intensities for all lines from the same upper level, with the lifetime. If experimental data are not available, one has to rely on theoretical calculations of the relative transition probabilities. For strong transitions, theoretical values are usually quite accurate but for weaker lines, where cancellation or intermediate coupling effects could be important, the accuracy of more of them is difficult to assess.

The ground term in neutral rhodium is the even $4d^8(^3F)5s\ a^4F$, and the ionization energy is 60 197 cm^{-1} (Moore 1958). The even electron configurations are well established up to the $4d^8(^3F)6s\ e^2F$ at 42 292 cm^{-1}. For most of the higher lying even states only the energy and *J*-values are given by Moore (Moore 1958). The lowest odd configuration, $4d^8(^3F)5p\ z^4D^o$, starts at an energy of 27 075 cm^{-1} and for most levels above 45 315 cm^{-1} only the energy and *J*-values are given. To the best of our knowledge, no theoretical investigations of the energy structure and decay properties in Rh I have been published.

There are three papers in the literature dedicated to the determination of radiative lifetimes and transition probabilities for low-lying odd states in Rh I. Kwiatkowski et al. (Kwiatkowski et al. 1982) report lifetime measurements for Nb I and Rh I using time-resolved laser-induced fluorescence (TR-LIF) on an atomic beam. The radiative lifetimes of 13 odd levels of Rh I, in the energy range 27 075–36 787 cm^{-1}, are reported in the paper. The measured lifetimes are combined with branching ratios from Corliss and Bozman (Corliss & Bozman 1962) to obtain oscillator strengths for a number of transitions. These improved *f*-values are then used to refine the solar abundance of rhodium. Salih et al. (Salih, Duquette & Lawler 1983) also used TR-LIF on an atomic beam to measure lifetimes in Rh I and Ta I. For rhodium, 22 radiative lifetimes for levels in the energy region 27 075–39 127 cm^{-1} are reported. The *A*-values of six Rh I spectral lines, which are important for the abundance determination of rhodium in the sun, are derived using the Corliss and Bozman data (Corliss & Bozman 1962). In an extended work, Duquette and Lawler (Duquette & Lawler 1985) studied the spectrum of neutral rhodium from a hollow cathode discharge, using the 1-m Fourier transform spectrometer at the National Solar Observatory in New Mexico, to obtain improved branching fractions and determined the absolute transition probabilities for 115 spectral lines.

In summary, the previous studies (Kwiatkowski et al. 1982; Corliss and Bozman 1962; Salih et al. 1983; Duquette & Lawler 1985) have determined radiative lifetimes and transition probabilities for odd states of Rh I having energies up to 39 100 cm^{-1}. The present paper extends the lifetime measurements by 13 high-lying odd states with energies between 37 300 and 46 500 cm^{-1}. In

⋆ E-mail: kblagoev@issp.bas.bg

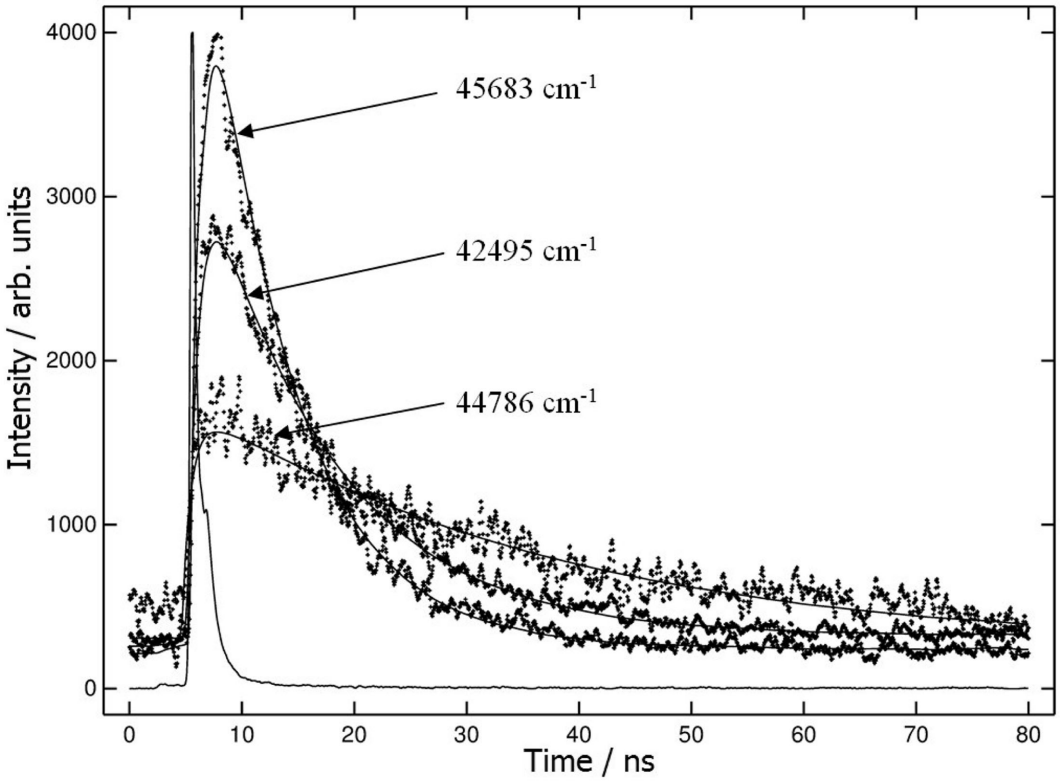

Figure 1. Lifetime measurements for Rh I. Crosses show the recorded decay curves for the levels 45 683 cm^{-1} (6.8 ns), 42 495 cm^{-1} (11.0 ns) and 44 786 cm^{-1} (31.0 ns). The solid lines show the fitted exponential decays and the measured pulse shape for the 45 683 cm^{-1} level. In all cases, the actual measurements extend to much longer times.

addition, we report the first detailed theoretical investigation of the decay properties of the experimentally established energy levels using a pseudo-relativistic Hartree–Fock (HFR) model including core-polarization effects.

2 EXPERIMENT

The experimental set-up for TR-LIF experiments at the Lund High Power Laser Facility has previously been discussed in detail by Bergström et al. (1988) and, more recently, by Engström et al. (2014). Here we will only give a short description of the parameters relevant for the present experiment. Free rhodium atoms and ions were created in an ablation process by focusing a frequency doubled Nd:YAG laser (Continuum Surlite) at 532 nm onto a rotating rhodium target, placed in a vacuum chamber with a residual pressure of 10^{-5} mbar. The created atoms were excited by crossing the ablation plasma 1 cm above the target with the light emitted from a dye laser (Continuum Nd 60), operating with DCM dye. The dye laser was pumped by an injection seeded and Q-switched Nd:YAG laser (Continuum NY-82), where the pulses were temporally compressed using stimulated Brillouin scattering in water and had a duration of about 1.5 ns (full width at half-maximum, FWHM). The wavelengths necessary to excite the different states under investigation were obtained by frequency doubling or tripling in KDP and barium borate crystals. In addition, a Raman shifter, based on scattering in hydrogen gas, was used to add or subtract Stokes components of 4153 cm^{-1}. All lasers operated at 10 Hz and were synchronized by a pulse generator, which provided a variable delay between the ablation and excitation pulses.

The LIF signal was detected by a 1/8-m grating monochromator with its entrance slit oriented parallel to the excitation laser beam and perpendicular to the ablation laser. The LIF signal was registered by a fast micro-channel-plate photomultiplier tube (Hamamatsu R3809U) and digitized by a Tektronix DPO 7254 oscilloscope. The trigger pulse for the oscilloscope was taken from a fast photo-diode, which registered the temporal shape of the excitation pulse before it passed into the vacuum chamber. The decay curves were formed by averaging over 1000 laser pulses and transferred to a personal computer together with the measured excitation laser pulse. Typical decay curves for short, medium and long lifetimes are presented in Fig. 1.

The code DECFIT (Palmeri et al. 2008) was used to extract the experimental lifetimes from a least-squares fit of a single exponential decay, convoluted by the measured excitation pulse, and a constant background. For the Rh I excited states with sufficiently long lifetimes (typically three times the full width of the laser pulse), this convolution technique could be avoided and a single exponential fit using only the region after the excitation pulse sufficed.

The wavelengths and excitation schemes used in this work are presented in Table 1. As seen in this table, all but one of the investigated levels are excited from the even levels of the ground term, $4d^8(^3F)5s\ a^4F$, spanning an energy of 0–3500 cm^{-1}. $4d^8(^3P)5p\ z^4S_{3/2}$ was excited from $4d^8(^3P)5s\ a^4P_{5/2}$ at 9221 cm^{-1}. We have followed the *LS* notation used by Moore (Moore 1958) but it is clear by the violation of both the ΔL and ΔS selection rules that this is not a perfect representation. All but two of the transitions used are included in Meggers, Corliss & Scribner (1975) and Kramida, Ralchenko & Reader (2014). The excitation channels $4d^8(^3F)5s\ a^4F_{9/2}$–$4d^8(^1G)5p\ y^2G_{9/2}$ at 220.61 nm and $4d^8(^3F)5s$

Table 1. Excitation scheme for the studied levels in Rh I.

Level[a]	E[a]/cm^{-1}	Starting level[a] E/cm^{-1}	Excitation[b] λ_{air}/nm	Scheme[c] λ_{air}/nm	Detection[b]
4d^{8}5p z^{4}G°$_{7/2}$	31 101.75	0	321.43	2ω	360, 393
4d^{8}5p z^{2}D°$_{3/2}$	33 867.04	2598.03	319.71	2ω	354, 383
4d^{8}5p z^{4}P°$_{5/2}$	35 333.85	3472.68	313.77	2ω	383, 400
4d^{8}5p y^{4}D°$_{7/2}$	36 787.48	1529.97	283.54	2ω	415
4d^{8}5p z^{4}S°$_{3/2}$	40 900.00	9221.22	315.58	2ω	334, 377
12° $J = 9/2$	41 953.07	0	238.29	3ω+S	342, 387
13° $J = 9/2$	42 325.46	0	236.19	3ω+S	338, 382
14° $J = 7/2$	42 495.48	0	235.25	3ω+S	244, 345, 361,[d] 377
15° $J = 9/2$	43 042.31	0	232.26	3ω+S	232, 371
16° $J = 7/2$	43 047.54	1529.97	240.79	3ω+S	252, 370
4d^{8}5p x^{2}D°$_{5/2}$	43 421.40	1529.97	238.64[d]	3ω+S	250, 366
4d^{8}5p x^{2}F°$_{7/2}$	43 904.73	1529.97	235.92	3ω+S	288
17° $J = 7/2$	44 588.12	1529.97	232.17	3ω+S	283
19° $J = 5/2$	44 786.67	3472.68	241.97	3ω+S	290
4d^{8}5p y^{2}G°$_{9/2}$	45 315.54	0	220.61[d]	3ω	307, 341
20° $J = 5/2$	45 683.41	3472.68	236.83	3ω+S	274, 283
21° $J = 3/2$	46 280.09	2598.03	228.86	3ω+S	278, 283

Notes. [a]Moore 1958.
[b]Kramida et al. 2014.
[c]2ω and 3ω are the second and third harmonics of the dye laser and S is one added Stokes shift of 4153 cm^{-1}.
[d]Not observed by Kramida et al. 2014, but exist in tables of spectral lines (Harrison 1969).

a^{4}F$_{7/2}$ -4d^8(^{1}D)5p x^{2}D$_{5/2}$ at 238.64 nm are reported for the first time in this work. These lines are verified in unpublished Fourier transform spectra recorded with the Chelsea FT500 instrument at Lund Observatory. Although we only used one channel to excite the different levels, in most cases the fluorescence was detected at several wavelengths to check the identifications and to avoid possible blends or spectral coincidences.

To investigate any systematic influence on the lifetimes from radiation trapping, collisional deexcitation or time-of-flight effect, the delay between the ablation and excitation pulses was varied in a wide interval from 1.7 to 5.0 μs. To test for possible saturation effects, a set of neutral density filters was placed in the excitation laser beam. No systematic effects were found. The experimental lifetimes obtained in the present work are presented in Table 2. The values represent the averages of about 20 measurements under the different conditions mentioned above and using different detection channels. The quoted uncertainties in the lifetimes include the statistical uncertainties as well as the variation of the results between the repeated measurements.

3 CALCULATIONS

The computational approach considered in the present work is the pseudo-relativistic HFR method of Cowan (1981), in which we have incorporated the core-polarization effects, as described in many of our previous papers, see e.g. Quinet et al. (1999, 2002). The configurations included in the calculations were 4d^{8}5s, 4d^{8}6s, 4d^{8}5d, 4d^{8}6d, 4d^9, 4d^{7}5s^2, 4d^{7}5p^2, 4d^{7}5d^2, 4d^{7}5s6s, 4d^{7}5s5d, 4d^{7}5s6d for the even parity, and 4d^{8}5p, 4d^{8}6p, 4d^{8}4f, 4d^{8}5f, 4d^{7}5s5p, 4d^{7}5s6p, 4d^{7}5p5d, 4d^{7}5p6s for the odd parity. The estimate of the core-polarization contributions requires knowledge of the dipole polarizability of the ionic core, α_d, and of the cut-off radius, r_c. For the first parameter, we used the value of the static dipole polarizability computed by Fraga, Karwowski & Saxena (1976) for Rh III, i.e. $\alpha_d = 7.42a_0^3$. The cut-off radius, r_c, was chosen equal to $1.50a_0$, which corresponds to the HFR average value, $<r>$, of the outermost core orbitals 4d.

Table 2. Radiative lifetimes for Rh I.

Level[a]	E[a]/cm^{-1}	Lifetime/ns Experiment This work	Experiment Previous	Theory This work
4d^{8}5p z^{4}D°$_{7/2}$	27 075.26		10.4 ± 0.5[b]	9.9
			10.6 ± 0.5[c]	
4d^{8}5p z^{4}G°$_{9/2}$	28 542.69		9.7 ± 0.5[b]	9.3
			10.1 ± 0.5[c]	
4d^{8}5p z^{4}D°$_{5/2}$	28 859.64		10.4 ± 0.5[c]	9.4
4d^{8}5p z^{4}G°$_{11/2}$	29 104.71		7.5 ± 0.4[b]	7.3
4d^{8}5p z^{4}F°$_{9/2}$	29 430.86		9.2 ± 0.5[b]	9.0
			9.2 ± 0.5[c]	
4d^{8}5p z^{4}F°$_{7/2}$	29 866.34		9.5 ± 0.5[c]	8.7
4d^{8}5p z^{4}D°$_{3/2}$	30 397.27		10.2 ± 0.5[c]	9.5
4d^{8}5p z^{4}G°$_{7/2}$	31 101.75	9.2 ± 0.4	9.2 ± 0.5[b]	8.7
			8.6 ± 0.4[c]	
4d^{8}5p z^{4}D°$_{1/2}$	31 146.68		10.1 ± 0.5[b]	9.4
			10.1 ± 0.5[c]	
4d^{8}5p z^{4}F°$_{5/2}$	31 474.50		8.6 ± 0.4[b]	8.4
			9.0 ± 0.5[c]	
4d^{8}5p z^{2}G°$_{9/2}$	31 613.78		8.2 ± 0.4[c]	8.3
4d^{8}5p z^{2}F°$_{7/2}$	32 004.01		9.4 ± 0.5[b]	9.2
			8.7 ± 0.4[c]	
4d^{8}5p z^{2}D°$_{5/2}$	32 046.32		8.1 ± 0.4[c]	8.5
4d^{8}5p z^{4}G°$_{5/2}$	32 243.32		7.7 ± 0.4[b]	7.4
4d^{8}5p z^{4}F°$_{3/2}$	32 277.43		9.5 ± 0.5[b]	9.1
			8.7 ± 0.4[c]	
4d^{8}5p z^{2}G°$_{7/2}$	33 043.91		8.9 ± 0.4[b]	8.9
			9.2 ± 0.5[c]	
4d^{8}5p z^{2}D°$_{3/2}$	33 867.04	7.7 ± 0.4	7.6 ± 0.4[b]	7.6
			7.0 ± 0.3[c]	
4d^{8}5p z^{2}F°$_{5/2}$	33 946.34		7.3 ± 0.4[c]	7.6
4d^{8}5p z^{4}P°$_{5/2}$	35 333.85	11.6 ± 0.5	12.0 ± 0.6[c]	11.3
4d^{8}5p z^{4}P°$_{3/2}$	35 404.24		9.8 ± 0.5[c]	9.7
4d^{8}5p z^{4}P°$_{1/2}$	35 669.50		12.2 ± 0.6[c]	11.8
4d^{8}5p y^{4}D°$_{7/2}$	36 787.48	11.0 ± 0.5	10.3 ± 0.6[b]	10.8
			11.3 ± 0.6[c]	

Table 2. – *continued*

Level[a]	E[a]/cm^{-1}	Lifetime/ns		
		Experiment		Theory
		This work	Previous	This work
$4d^8 5p\ y^4D^\circ_{1/2}$	38 474.43		17.1 ± 0.9[c]	12.8
$6^\circ\ J = 5/2$	39 126.76		16.0 ± 0.8[c]	15.3
$4d^8 5p\ z^4S^\circ_{3/2}$	40 900.00	7.9 ± 0.4		7.4
$12^\circ\ J = 9/2$	41 953.07	14.8 ± 1.0		14.5
$13^\circ\ J = 9/2$	42 325.46	9.9 ± 0.4		10.3
$14^\circ\ J = 7/2$	42 495.48	11.0 ± 0.5		11.5
$15^\circ\ J = 9/2$	43042.31	18.1 ± 1.0		19.2
$16^\circ\ J = 7/2$	43 047.54	7.3 ± 0.4		7.1
$4d^8 5p\ x^2D^\circ_{5/2}$	43 421.40	8.6 ± 0.4		7.6
$4d^8 5p\ x^2F^\circ_{7/2}$	43 904.73	18 ± 1		19.2
$17^\circ\ J = 7/2$	44 588.12	6.7 ± 0.3		7.3
$19^\circ\ J = 5/2$	44 786.67	31.0 ± 2.0		28.8
$4d^8 5p\ y^2G^\circ_{9/2}$	45 315.54	7.8 ± 0.4		7.5
$20^\circ\ J = 5/2$	45 683.41	6.8 ± 0.3		7.0
$21^\circ\ J = 3/2$	46 280.09	6.4 ± 0.3		6.9

Notes. [a]Moore 1958.
[b]Kwiatkowski et al. 1982, TR-LIF technique using an atomic beam.
[c]Salih et al. 1983, TR-LIF technique using an atomic beam.

Some of the radial integrals were adjusted in a least-squares-fit procedure, minimizing the discrepancies between the Hamiltonian eigenvalues and the experimental energy levels taken from Moore's compilation (Moore 1958). For some highly excited levels, typically above 47 000 cm^{-1} in both parities, we could not establish an unambiguous connection between the experimental and calculated values so those levels were omitted in the semi-empirical process. More precisely, in the even-parity system, 32 experimental levels were used to optimize the configuration average energies ($E_{\rm av}$), the electrostatic Slater integrals (F^k, G^k), the spin-orbit parameters (ζ_{nl}) and the effective interaction parameters (α) in the $4d^8 5s$, $4d^9$ and $4d^7 5s^2$ configurations. Due to the limited number of experimentally identified terms belonging to $4d^8 6s$, only $E_{\rm av}$ and ζ_{4d} were adjusted in this configuration. Regarding the odd-parity configurations, 66 experimental levels were used to optimize the $E_{\rm av}$, F^k, G^k, ζ_{nl} and α parameters belonging to the $4d^8 5p$ and $4d^7 5s5p$ configurations. The parameters not included in the fitting procedures were held fixed at 80 per cent of their HFR *ab initio* values.

The calculated energies and dominating eigenvector components for the even-parity levels are given in Table 3. Compared to the energies and *LS* designations given by Moore (1958), we find an average energy deviation of 35 cm^{-1} and confirm all level designations except a suggested exchange of the $^2F_{5/2}$ and $^4F_{5/2}$ labels for the levels at 44 474 and 45 471 cm^{-1}. Table 4 gives a similar comparison for the odd-parity levels. In this case the average energy deviation is 43 cm^{-1} and the level mixing is more severe. However, for levels below 38 000 cm^{-1}, we again confirm the *LS* designations given by Moore (1958). For higher energies it is difficult to give any meaningful names at all, and we note, for example, that the calculated eigenvector representations for the levels at 40 900, 43 421 and 43 904 cm^{-1}, for which we have measured the lifetimes, do not support the designations by Moore (1958) given in Table 2.

Table 3. Theoretical and experimental energies for even-parity levels up to 47 000 cm^{-1}. (The full table is available online.)

$E^{\rm a}_{\rm exp}$/cm^{-1}	$E^{\rm b}_{\rm theory}$/cm^{-1}	ΔE/cm^{-1}	J	*LS* composition (percentage)[b,c]
0.00	−8	8	4.5	98 $4d^8(^3F)5s\ ^4F$
1529.97	1506	24	3.5	92 $4d^8(^3F)5s\ ^4F$ + 6 $4d^8(^3F)5s\ ^2F$
2598.03	2625	−27	2.5	56 $4d^8(^3F)5s\ ^4F$ + 33 $4d^{92}D$ + 9 $4d^8(^1D)5s\ ^2D$
3309.86	3291	19	2.5	50 $4d^{92}D$ + 40 $4d^8(^3F)5s\ ^4F$
3472.68	3490	−17	1.5	81 $4d^8(^3F)5s\ ^4F$ + 10 $4d^8(^1D)5s\ ^2D$ + 7 $4d^{92}D$
5657.97	5655	3	1.5	72 $4d^{92}D$ + 14 $4d^8(^3F)5s\ ^4F$ + 11 $4d^8(^1D)5s\ ^2D$
5690.97	5680	11	3.5	90 $4d^8(^3F)5s\ ^2F$ + 7 $4d^8(^3F)5s\ ^4F$
7791.23	7813	−22	2.5	77 $4d^8(^3F)5s\ ^2F$ + 8 $4d^8(^1D)5s\ ^2D$ + 7 $4d^8(^3P)5s\ ^4P$
9221.22	9242	−21	2.5	78 $4d^8(^3P)5s\ ^4P$ + 12 $4d^8(^3F)5s\ ^2F$ + 5 $4d^8(^1D)5s\ ^2D$

Notes. [a]Moore 1958.
[b]This work.
[c]Only the first three eigenvector components are given, if they are greater than 5 per cent.

Table 4. Theoretical and experimental energies for odd-parity levels up to 47 000 cm^{-1}. (The full table is available online.)

$E^{\rm a}_{\rm exp}$/cm^{-1}	$E^{\rm b}_{\rm theory}$/cm^{-1}	ΔE/cm^{-1}	J	*LS* composition (percentage)[b,c]
27 075.26	27 103	−28	3.5	85 $4d^8(^3F)5p\ ^4D$ + 6 $4d^8(^3F)5p\ ^4F$
28 542.69	28 557	−14	4.5	34 $4d^8(^3F)5p\ ^4G$ + 33 $4d^8(^3F)5p\ ^2G$ + 29 $4d^8(^3F)5p\ ^4F$
28 859.64	28 858	2	2.5	79 $4d8(^3F)5p\ ^4D$ + 5 $4d^8(^3F)5p\ ^4F$
29 104.71	29 110	−5	5.5	97 $4d8(^3F)5p\ ^4G$
29 430.86	29 375	56	4.5	58 $4d8(^3F)5p\ ^4F$ + 33 $4d^8(^3F)5p\ ^2G$
29 866.34	29 818	48	3.5	41 $4d^8(^3F)5p\ ^4F$ + 26 $4d^8(^3F)5p\ ^2F$ + 16 $4d^8(^3F)5p\ ^4G$
30 397.27	30 370	27	1.5	85 $4d^8(^3F)5p\ ^4D$
31 101.75	31 138	−36	3.5	57 $4d^8(^3F)5p\ ^4G$ + 21 $4d^8(^3F)5p\ ^2F$ + 14 $4d^8(^3F)5p\ ^2G$
31 146.68	31 127	20	0.5	85 $4d^8(^3F)5p\ ^4D$ + 5 $4d^8(^3P)5p\ ^4D$

Notes. [a]Moore 1958.
[b]This work.
[c]Only the first three eigenvector components are given, if they are greater than 5 per cent.

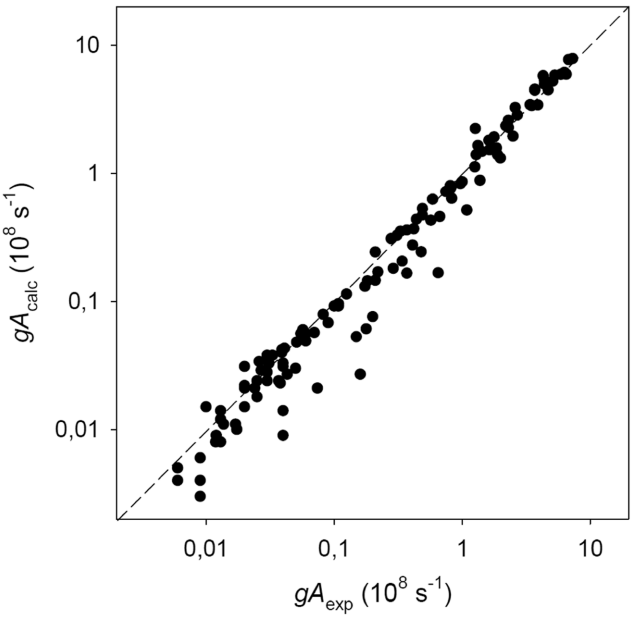

Figure 2. Comparison between the calculated transition probabilities obtained in the present work (gA_{calc}) and the experimental values (gA_{exp}) reported by Duquette & Lawler (1985).

4 DISCUSSION

Table 2 presents the experimental and theoretical lifetimes obtained in this work as well as the experimental values from the previous investigations (Kwiatkowski et al. 1982; Salih et al. 1983). Four of the levels have been measured in all three experimental studies and we note a good agreement in all cases. The only exception occurs for the $4d^8 5p\ y^4D_{1/2}$ level at 38 474.43 cm^{-1} for which our calculated lifetime (12.8 ns) is a factor of 1.3 shorter than the measurement (17.1 ns). This level is mainly depopulated by two dominant transitions to the even-parity levels situated at 11 006.5 cm^{-1} ($J = 1/2$) and 11 968.23 cm^{-1} ($J = 3/2$). The first is characterized by a rather pure *LS* wavefunction (97 per cent) but this is not the case for the second, which appears very strongly mixed in our calculations (see Table 3). This could explain the higher sensitivity of the corresponding transition probability to the upper odd-parity state, and therefore its computed lifetime.

If we compare our calculated lifetimes with the experimental values obtained in this work and those measured previously (Kwiatkowski et al. 1982; Salih et al. 1983), we find again an excellent agreement for all the levels considered. The difference between the experimental and theoretical results is typically less than 5 percent, and well within the experimental uncertainties. In Fig. 2, we compare the transition probabilities deduced from our calculations and the results published by Duquette and Lawler (1985), who combined branching fractions measured on Fourier-transform spectra with the experimental lifetimes (Kwiatkowski et al. 1982; Salih et al. 1983) to determine *gA*-values for 115 lines depopulating Rh I levels between 27 075 and 35 670 cm^{-1}. As seen in this figure, the overall agreement between computed and experimental transition probabilities is good. The average ratio between the two sets of data is $<gA_{calc}/gA_{exp}> = 0.88 \pm 0.27$, where the uncertainty represents the standard deviation from the mean. It is worth noting that this ratio becomes 0.94 ± 0.24 and 1.06 ± 0.20 when only $gA_{calc} \geq 10^7\ s^{-1}$ or $gA_{calc} \geq 10^8\ s^{-1}$ respectively, are retained in the mean, showing that our calculated transition probabilities can be expected to be reliable to within 10–20 per cent for the stronger lines. In Table 5, we give the computed oscillator strengths and transition probabilities obtained in the present work for Rh I lines involving energy levels below 47 000 cm^{-1} and with *gA*-values greater than $10^7\ s^{-1}$. This corresponds to 308 radiative transitions appearing in the spectral region between 2200 and 10 000 Å.

Table 5. Oscillator strengths (log *gf*) and transition probabilities (*gA*) for Rh I lines. (The full table is available online.)

λ/Å[a]	Lower level[b]		Upper level[b]		This work[c]		Other[d]
	E/cm^{-1}	J	E/cm^{-1}	J	log gf	gA/s^{-1}	gA/s^{-1}
2206.060	0	4.5	*45 316*	4.5	−1.85	1.95×10^7	
2212.795	0	4.5	*45 178*	3.5	−1.47	4.63×10^7	
2242.054	0	4.5	*44 588*	3.5	−0.29	6.87×10^8	
2264.129	1530	3.5	*45 683*	2.5	−0.34	5.97×10^8	
2276.956	0	4.5	*43 905*	3.5	−0.97	1.38×10^8	
2288.563	2598	2.5	*46 280*	1.5	−0.79	2.06×10^8	
2309.816	3473	1.5	*46 753*	0.5	−0.98	1.31×10^8	
2311.070	1530	3.5	*44 787*	2.5	−1.59	3.24×10^7	
2318.370	5691	3.5	*48 811*	3.5	−1.33	5.75×10^7	

Notes. [a]Air wavelengths deduced from experimental energy levels.
[b]From Moore 1958. Odd-parity energies are in italics.
[c]Calculated values obtained in the present work. Estimated uncertainties within 10–20 per cent (see text).
[d]Duquette & Lawler 1985.

ACKNOWLEDGEMENTS

This work has received funding from LASERLAB-EUROPE (grant agreement 284464, EC's Seventh Framework Programme), the Swedish Research Council through the Linnaeus grant to the Lund Laser Centre and a project grant 621-2011-4206, and the Knut and Alice Wallenberg Foundation. PP and PQ are respectively a research associate and a research director of the Belgian National Fund for Scientific Research (FRS-FNRS), from which financial support is gratefully acknowledged. GM and KB are grateful to their colleagues at the Lund Laser Centre for their kind hospitality and support.

REFERENCES

Bergström H., Faris H., Hallstadius G. W., Lundberg H., Persson A., Wahlström C. G., 1988, Z. Phys. D, 8, 17
Cameron A. G. W., 1981, in Barnes C. A., Clayton D. D., Schramm D. N., eds, Essays in Nuclear Astrophysics. Cambridge Univ. Press, p. 23
Corliss C. H., Bozman W. R., 1962, NBS Monograph 53, Washington, DC
Cowan R. D., 1981, The Theory of Atomic Structure and Spectra, Univ. California Press, Berkeley (USA)
Duquette D. W., Lawler J. L., 1985, J. Opt. Soc. America, 12, 1948
Engström L., Lundberg H., Nilsson H., Hartman H., Bäckström E., 2014, A&A, 570, A34
Fraga S., Karwowski J., Saxena K. M., 1976, Handbook of Atomic Data. Elsevier, Amsterdam
Harrison G. R., 1969, Wavelength Tables, MIT Press
Kramida A., Ralchenko Yu., Reader J., 2014, NIST Atomic Spectra Database. Available: http://physics.nist.gov/asd
Kwiatkowski M., Zimmermann P., Biémont É., Grevesse N., 1982, Astron. Astrophys., 112, 337
Meggers W. F., Corliss C. H., Scribner B. F., 1975, Tables of Spectral-Line Intensities, Part I–Arranged by Elements, Part II–Arranged by Wavelengths, Nat. Bur. Stand Monograph 145, US, p. 600

Moore C. E., 1958, Atomic Energy Levels, Vol. III, Natl. Bur. Stand. (US), Circ. 467. US Government Printing Office, Washington DC
Palmeri P., Quinet P., Fivet V., Biémont É, Nilsson H., Engström L., Lundberg H., 2008, Physica Scripta, 78, 015304
Quinet P., Palmeri P., Biémont É., McCurdy M. M., Rieger G., Pinnington E. H., Wickliffe M. E., Lawler J. E., 1999, MNRAS, 307, 934
Quinet P., Palmeri P., Biémont É., Li Z. S., Zhang Z. G., Svanberg S., 2002, Alloys Comp., 344, 255
Salih S., Duquette D. W., Lawler J. E., 1983, Phys. Rev., A27, 1193

SUPPORTING INFORMATION

Additional Supporting Information may be found in the online version of this article:

Table 3. Theoretical and experimental energies for even-parity levels up to 47 000 cm^{-1}.

Table 4. Theoretical and experimental energies for odd-parity levels up to 47 000 cm^{-1}.

Table 5. Oscillator strengths (log *gf*) and transition probabilities (*gA*) for Rh I lines.

(http://mnras.oxfordjournals.org/lookup/suppl/doi:10.1093/mnras/stv375/-/DC1)

Please note: Oxford University Press is not responsible for the content or functionality of any supporting materials supplied by the authors. Any queries (other than missing material) should be directed to the corresponding author for the article.

This paper has been typeset from a TEX/LATEX file prepared by the author.